Electronic Supplementary Information (ESI)

CoO-modified Co_4N as a heterostructure electrocatalyst for highly efficient overall water splitting in neutral media

Rui-Qing Li,[a] Pengfei Hu,[b] Meng Miao,[a] Yongle Li,[b] Xiang-Fen Jiang,[*c] Qiang Wu,[d] Zhen Meng,[e] Zheng Hu,[d] Yoshio Bando[c,f] and Xue-Bin Wang[*a]

[a] National Laboratory of Solid State Microstructures, Collaborative Innovation Center of Advanced Microstructures, College of Engineering and Applied Sciences, Nanjing University, Nanjing 210093, China. E-mail: wangxb@nju.edu.cn

[b] Department of Physics, International Center of Quantum and Molecular Structures, Shanghai University, Shanghai 200444, China.

[c] International Center for Materials Nanoarchitectonics (MANA), National Institute for Materials Science (NIMS), Tsukuba 3050044, Japan. E-mail: jiangxiangfen@gmail.com

[d] Key Laboratory of Mesoscopic Chemistry of Ministry of Education, School of Chemistry and Chemical Engineering, Nanjing University, Nanjing 210093, China.

[e] School Instrument Center, School of Chemistry and Chemical Engineering, Nanjing University, Nanjing 210093, China.

[f] Australian Institute for Innovative Materials, University of Wollongong, North Wollongong, NSW 2500, Australia.

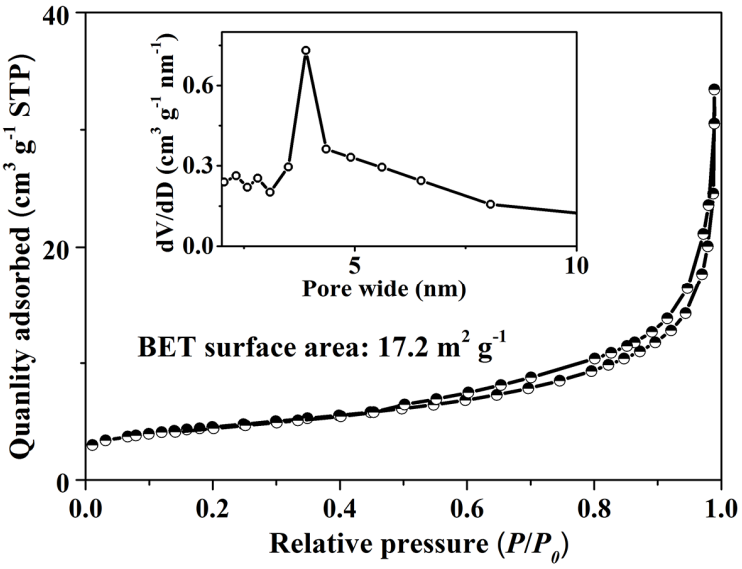

Figure S1. N_2 adsorption-desorption isotherm of CoO/Co_4N. Inset is the corresponding pore size distribution. The Brunauer-Emmett-Teller (BET) surface area of CoO/Co_4N is 17.2 m^2 g^{-1}, indicating its porous structure.

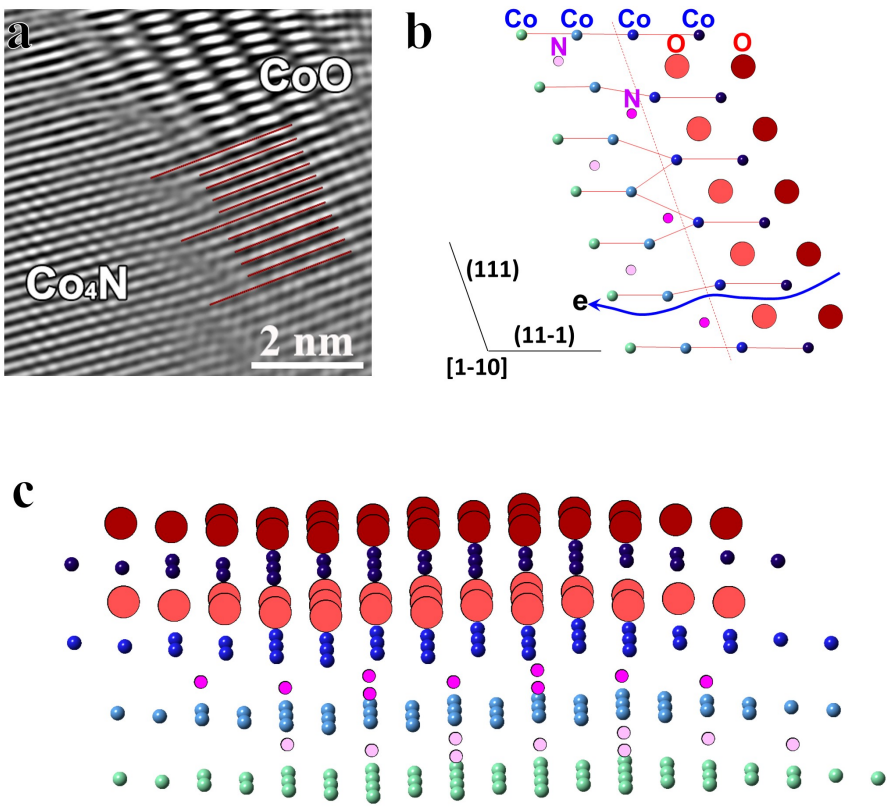

Figure S2. (a) HRTEM image *via* inverse fast Fourier transform filtering of Figure 1g. (b,c) Proposed structures with periodically aligned [11-1] planes every 6 spacings of Co_4N or 5 spacings of CoO, viewed at [1-10] and [-47-4] directions, respectively. The spacing of {111} of Co_4N is calculated to be 0.2053 nm from XRD in Figure 1e, which is *ca.* 5/6 the {111} spacing of CoO (0.24602 nm according to JCPDS 41-0943). This configuration can contribute a smooth electron transport through the interface.

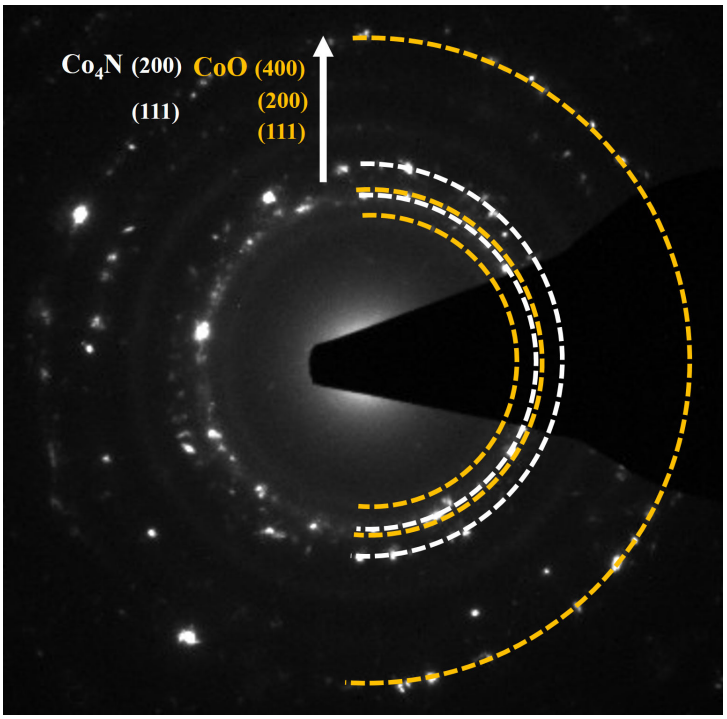

Figure S3. The SAED pattern of CoO/Co_4N.

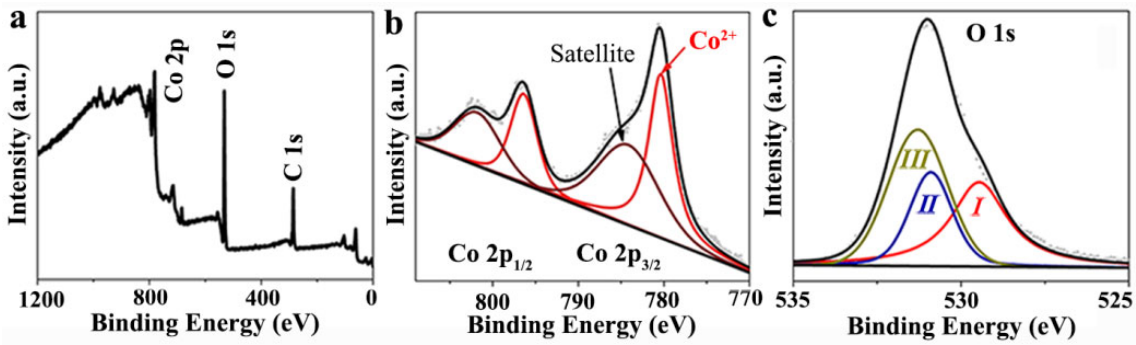

Figure S4. XPS spectra of (a) survey, (b) cobalt, and (c) oxygen scans of Co(OH)F.

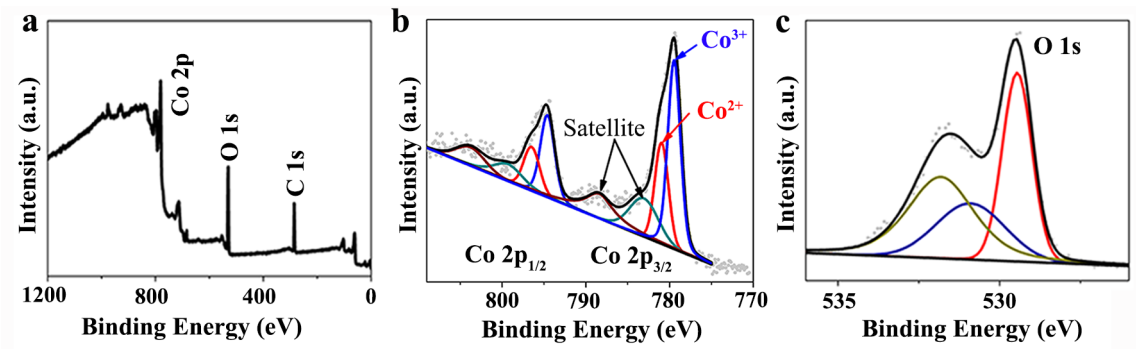

Figure S5. XPS spectra of (a) survey scan, (b) cobalt, and (c) oxygen scans of Co_3O_4.

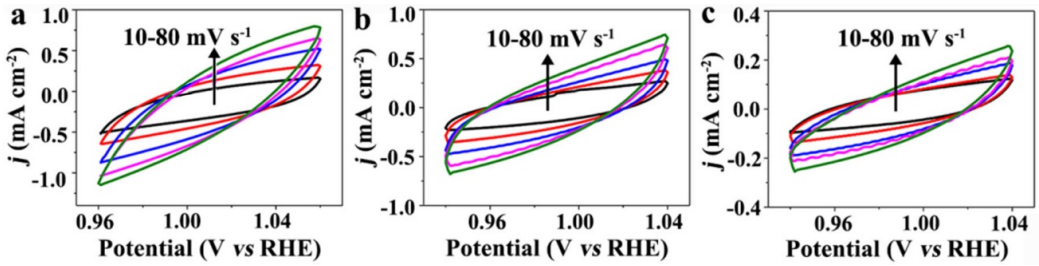

Figure S6. CV curves of (a) CoO/Co_4N, (b) Co_3O_4, and (c) Co(OH)F on NF at scan rates of 10-80 mV s^{-1} in 1 M PBS.

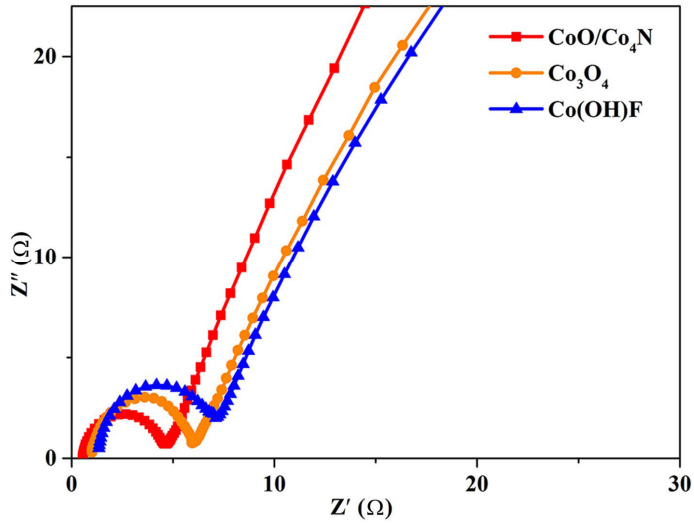

Figure S7. EIS curves of CoO/Co_4N, Co_3O_4 and Co(OH)F. CoO/Co_4N has the lowest low-frequency intercept (0.61 Ω) at horizontal axis, and the smallest diameter braced by the semicircle (4.04 Ω). They illuminate the enhanced conductivity and catalytic activity in CoO/Co_4N, respectively, for electrocatalysis.

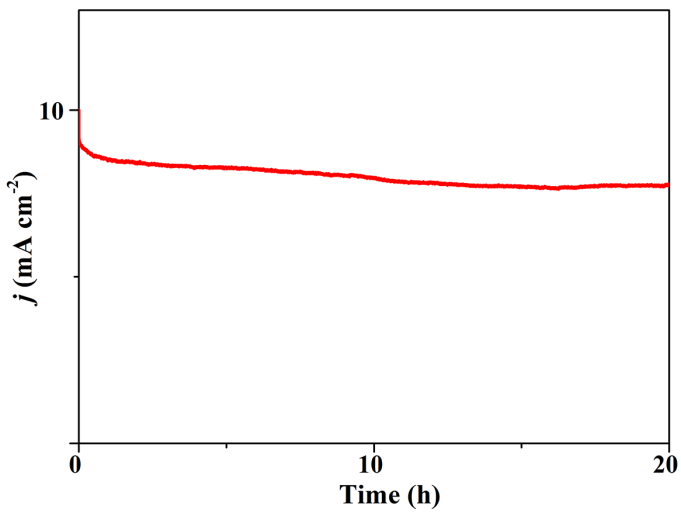

Figure S8. Chronoamperometric curve of the OER of CoO/Co_4N with a current of 10 mA cm^{-2}.

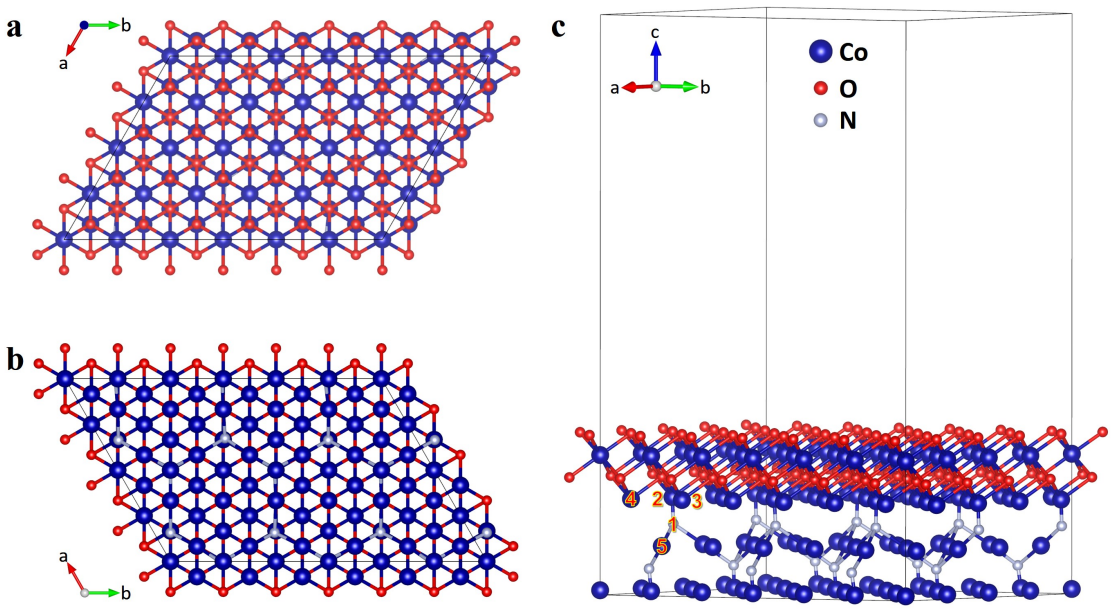

Figure S9. Constructed structure of CoO/Co_4N heterojunction: (a) top, (b) bottom, and (c) side views, respectively.

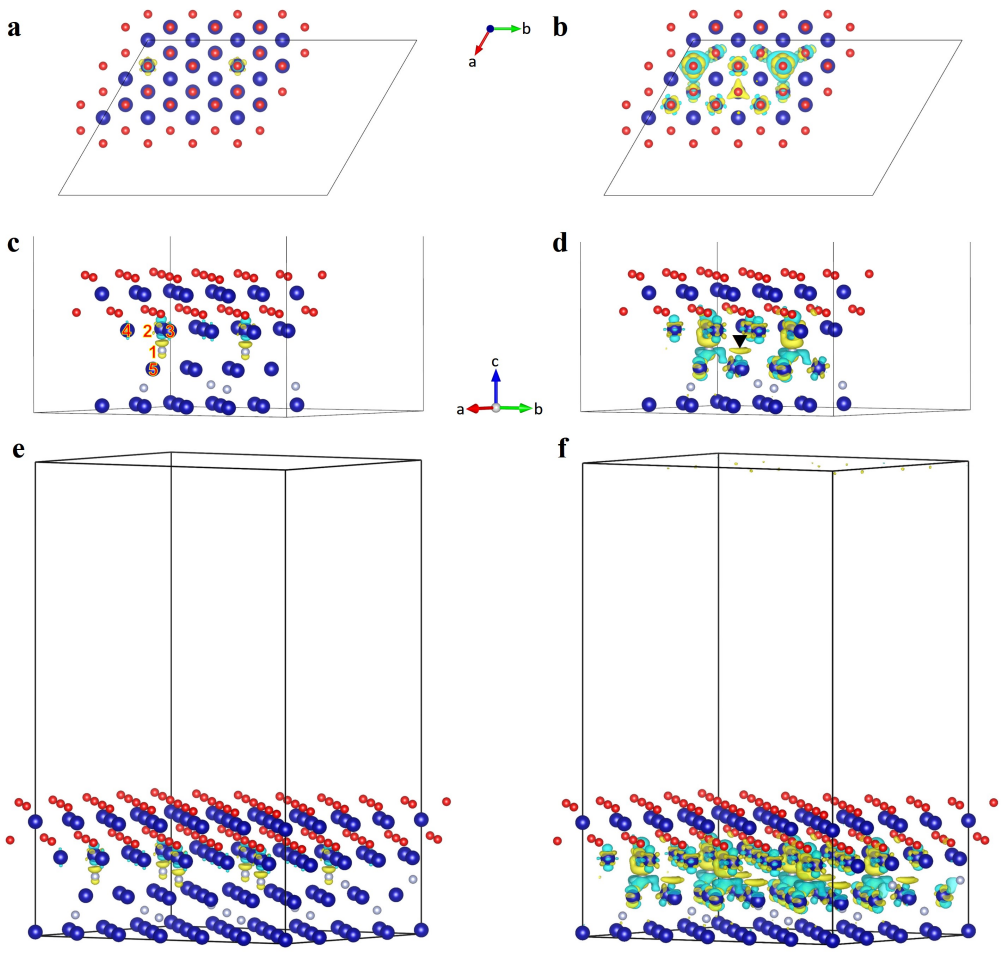

Figure S10. (a,b) Top and (c-f) side views of charge density difference of CoO/Co_4N *via* the subtraction between charge densities before and after meeting CoO and Co_4N, drawn at isosurfaces of 0.025 and 0.005 e $Bohr^{-3}$, respectively. The total amount of atoms in (a-d) is reduced by four for clear diagram. Yellow regions represent electron accumulation, and cyan ones represent consumption. There exists some electron decrement at cobalt atoms, and some accumulation at nitrogen atoms at the interface. The nitrogen-nearest neighbor, cobalt labeled as Co-2, contributes a large fraction of the electron transfer from cobalt to nitrogen (the residual electrons of Co-2 perform shrinkage as shown by some interspersed yellow regions). The nitrogen-next-nearest neighbors, cobalts labeled as Co-3 and Co-4, also contribute to the electron transfer from cobalt to nitrogen. For quantification, the net formal charges are -0.77, -0.57, -0.57, -0.36 and 0.69 for Co-2, 3, 4, 5, and N-1, respectively, according to the calculated Bader charges. It is noticeable that the interfacial bonding has some delocalization figure, as indicated by a delocalized electron accumulation marked by ▼ in (d).

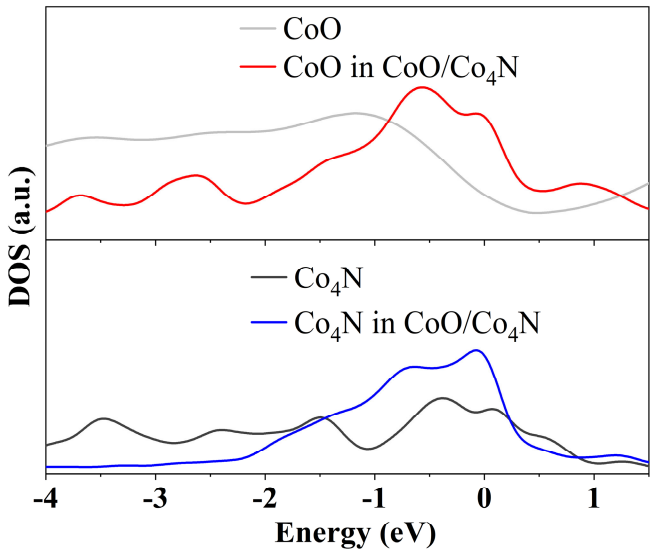

Figure S11. Partial DOS of CoO slab and Co_4N slab in CoO/Co_4N, as compared to DOS of pure phases CoO and Co_4N, respectively, indicating the mutual regulation of electron structures. Both partial DOS of CoO and Co_4N in CoO/Co_4N have clear increases around Fermi level, contributing to improving conductivity. The band modulation results from the interfacial coupling. Moreover, there is a DOS local peak for CoO slab in CoO/Co_4N at Fermi level. It implies that such CoO is more active for electron transfer benefiting electrocatalysis.[S1]

Table S1. Constituents of Co(OH)F, Co_3O_4, and CoO/Co_4N according to XPS. The nitrogen fraction of CoO/Co_4N is higher than the stoichiometric number owing to popular overestimation to light elements.

Samples	Co $2p_{3/2}$ (binding energy, eV | *atomic fraction, %*)						Lattice oxygen		Chemisorbed oxygen				Co:O in oxides	Co:N in nitride
	Co^0		Co^{3+}		Co^{2+}		Peak *I*		Peak *II*		Peak *III*			
Co(OH)F	-	-	-	-	780.4	*100*	529.5	*36*	530.9	*23*	531.6	*41*	0.97:1	-
Co_3O_4	-	-	779.3	*65*	780.9	*35*	529.5	*35*	530.9	*24*	531.8	*41*	0.70:1	-
CoO/Co_4N	779.2	*33*	-	-	780.8	*67*	529.5	*18*	530.9	*32*	531.7	*50*	1.05:1	2.1:1

Table S2. Comparison of OER activity of catalysts in neutral media in this work and recent reports.

Catalysts	η at 10 mA cm^{-2} (mV)	Tafel slop (mV dec^{-1})	Current density at 1.8 V (mA)	References
$CoO/Co_4N/NF$	**398**	**83**	**102**	**This work**
a-Co_2P	592	94.4	-	25
Cobalt borate	-	160	14.4	26
Cobalt phosphate	450	187	27	27
S-$NiFe_2O_4$/NF	494	118.1	-	31
$Co_{1-x}Fe_xP$/CNT	500	-	-	S2
FeNi-P	429	136	-	S3
Co_3S_4	-	151	2.4	S4
$Co(CO_3)_{0.5}(OH)\cdot 0.11H_2O$	460	284	-	S5
Mn_5O_8	-	-	5	S6
Co_3O_4/SWNT	-	-	6	S7
Fe-based film	-	-	5.6	S8
$Co(PO_3)_2$	590	74.1	-	S9
$ZnCo_2O_4$	-	76	2.7	S10

Table S3. Comparison of HER activity of catalysts in neutral media in this work and recent reports.

Catalysts	η at 10 mA cm^{-2} (mV)	Tafel slop (mV dec^{-1})	References
CoO/Co_4N/NF	**145**	**80**	**This work**
Co-NRCNTs	540	-	50
S-$NiFe_2O_4$/NF	197	81.3	31
SiO_2/PPy/NTs	>180	100.2	S11
Co-C-N	273	107	S12
Co-SNP/CC	74	111	S13
Co_9S_8	175	-	S14
H_2-CoCat	>385	140	S15
WP_2	244	92	S16
CoP/NF	180	189	S17
CoP	106	93	S18
$Ni_{1-x}Co_xSe_2$	82	78	S19
Cobalt sulfide	160	93	S20
FeP nanorod	202	71	S21
MoS_2/N-doped graphene	261	230	S22

Table S4. Comparison of overall water splitting of bifunctional catalysts in neutral media in this work and state-of-the-art reports.

Catalysts	Cell voltage at 10 mA cm^{-2} (V)	Electrolyte	References
$CoO/Co_4N/NF$	**1.79**	**1.0 M PBS**	**This work**
Doped carbon/oxidized carbon cloth	>1.9	0.2 M PBS	28
$NiFeO_x$/carbon fiber paper	1.83	1 M K_2HPO_4/KH_2PO_4	29
$CoO/CoSe_2$/titanium mesh	2.18	0.5 M PBS	30
S-$NiFe_2O_4$/NF	1.95	1.0 M PBS	31

References

S1. Y. Wu, Q. Shi, Y. Li, Z. Lai, H. Yu, H. Wang and F. Peng, *J. Mater. Chem. A*, 2015, **3**, 1142-1151.

S2. X. Zhang, X. Zhang, H. M. Xu, Z. S. Wu, H. L. Wang and Y. Y. Liang, *Adv. Funct. Mater.*, 2017, **27**, 1606635.

S3. B. W. Zhang, Y. H. Lui, L. Zhou, X. H. Tang and S. Hu, *J. Mater. Chem. A*, 2017, **5**, 13329-13335.

S4. Y. W. Liu, C. Xiao, M. J. Lyu, Y. Lin, W. Z. Cai, P. C. Huang, W. Tong, Y. M. Zou and Y. Xie, *Angew.Chem. Int. Ed.*, 2015, **54**, 11231-11235.

S5. L. Cui, D. N. Liu, S. Hao, F. L. Qu, G. Du, J. Q. Liu, A. M. Asirie and X. P. Sun, *Nanoscale*, 2017, **9**, 3752-3756.

S6. D. Jeong, K. Jin, S. E. Jerng, H. M. Seo, D. H. Kim, S. H. Nahm, S. H. Kim and K. T. Nam, *ACS Catal.*, 2015, **5**, 4624-4628.

S7. J. Wu, Y. Xue, X. Yan, Yan, S. W. Chen and Y. Xie, *Nano Res.*, 2012, **5**, 521-530.

S8. M. X. Chen, Y. Z. Wu, Y. Z. Han, X. H. Lin, L. Sun, W. Zhang and R. Cao, *ACS Appl. Mater. Interfaces*, 2015, **7**, 21852-21859.

S9. H. S. Ahn and T. D. Tilley, *Adv. Funct. Mater.*, 2013, **23**, 227-233.

S10. T. W. Kim, M. A. Woo, M. Regis and K. S. Cho, *J. Phys. Chem. Lett.*, 2014, **5**, 2370-2374.

S11. J. X. Feng, H. Xu, S. H. Ye, G. F. Ouyang, Y. X. Tong and G. R. Li, *Angew. Chem. Int. Ed.*, 2017, **56**, 8120-8124.

S12. Z. L. Wang, X. F. Hao, Z. Jiang, X. P. Sun, D. Xu, J. Wang, H. X. Zhong, F. L. Meng and X. B. Zhang, *J. Am. Chem. Soc.*, 2015, **137**, 15070-15073.

S13. B. R. Liu, L. Zhang, W. L. Xiong and M. M. Ma, *Angew. Chem. Int. Ed.*, 2016, **55**, 6725-6729.

S14. L. L. Feng, M. H. Fan, Y. Y. Wu, Y. P. Liu, G. D. Li, H. Chen, W. Chen, D. J. Wang and X. X. Zou, *J. Mater. Chem. A*, 2016, **4**, 6860-6867.

S15. C. Saioa, H. Jonathan, J. Pierre-andre, F. Jennifer and F. Vincent, *Nature Mater.*, 2012, **11**, 802-807.

S16. Z. C. Xing, Q. Liu, A. M. Asiri and X. P. Sun, *ACS Catal.*, 2015, **5**, 145-149.

S17. Y. P. Zhu, Y. P. Liu, T. Z. Ren and Z. Y. Yuan, *Adv. Funct. Mater.*, 2015, **25**, 7337-7347.

S18. J. Q. Tian, Q. Liu, A. M. Asiri and X. P. Sun, *J. Am. Chem. Soc.*, 2014, **136**, 7587-7590.

S19. B. Liu, Y. F. Zhao, H. Q. Peng, Z. Y. Zhang, C. K. Sit, M. F. Yuen, T. R. Zhang, C. S. Lee and W. J. Zhang, *Adv. Mater.*, 2017, **29**, 1606521.

S20. Y. J. Sun, C. Liu, D. C. Grauer, J. Yano, J. R. Long, P. D. Yang and C. J. Chang, *J. Am. Chem. Soc.*, 2013, **135**, 17699-17702.

S21. Y. H. Liang, Q. Liu, A. M. Asiri, X. P. Sun and Y. L. Luo, *ACS Catal.*, 2014, **4**, 4065-4069.

S22. Y. Hou, B. Zhang, Z. H. Wen, S. M. Cui, X. R. Guo, Z. He and J. H. Chen, *J. Mater. Chem. A*, 2014, **2**, 13795-13800.